Trop J Nat Prod Res, October 2025; 9(10): 5077 - 5084
ISSN 2616-0684 (Print)
ISSN 2616-0692 (Electronic)

Tropical Journal of Natural Product Research

Available online at https://www.tjnpr.org

Original Research Article

Molecular Docking and Dynamics Simulation of *Holothuria scabra* In Non-Small Cell Lung Cancer Through Inhibition of EGFR and KRAS Pathways

Ikhwandi C. Nugraha[1]* and Ami Febriza[2]

[1]*School of Medicine, Faculty of Medicine and Health Sciences, Universitas Muhammadiyah Makassar, Makassar, Indonesia 90221*
[2]*Physiology Department, Faculty of Medicine and Health Sciences, Universitas Muhammadiyah Makassar, Makassar, Indonesia 90221*

ARTICLE INFO

Article history:
Received 15 September 2025
Revised 10 October 2025
Accepted 15 October 2025
Published online 01 November 2025

ABSTRACT

Non-small cell lung cancer (NSCLC) is one of the leading causes of cancer-related mortality worldwide, highlighting the urgent need for novel therapeutics to overcome resistance and improve patient outcomes. This study employed an *in silico* pipeline to evaluate the potential of bioactive compounds from *Holothuria scabra* as inhibitors of epidermal growth factor receptor (EGFR) and KRAS, which are key NSCLC drivers. Selected *H. scabra* compounds retrieved from PubChem were screened for toxicity using ProTox 3.0, docked with PyRx/AutoDock Vina against EGFR (PDB: 2ITY) and KRAS (PDB: 7LGI) with Lazertinib as a comparator; the top-ranked complexes were further analyzed through 100 ns molecular dynamics simulations in YASARA (AMBER14/TIP3P) to assess stability. Several *H. scabra* ligands demonstrated stronger docking affinities than Lazertinib (e.g., C3: EGFR ΔG = −9.4 kcal·mol; C4: KRAS ΔG = −8.7 kcal·mol), while toxicity predictions indicated that all compounds were nontoxic. Docking analysis further revealed that compounds C3, C5, and C8 exhibited stronger affinities toward EGFR, with C3 interacting with key binding residues (VAL726, LYS745, and ASP855). Compounds C4, C3, and C7 showed superior affinities for KRAS, with C4 binding to critical residues (LYS117 and LYS147), similar to Lazertinib. Molecular dynamics simulations confirmed that the top ligands, particularly C3 and C4, maintained stable interactions without inducing significant protein unfolding or persistent root mean square deviation fluctuations. These findings indicate that *H. scabra*-derived ligands, especially C3 and C4, represent promising *in silico* candidates for subsequent biochemical and cellular validation as potential NSCLC inhibitors.

Keywords: Non-Small Cell Lung Cancer, Molecular Docking, Molecular Dynamic, *Holothuria scabra*, Epidermal Growth Factor Receptor, Kirsten Rat Sarcoma Viral Oncogene Homolog

Introduction

Lung cancer is one of the deadliest diseases and has become a major health concern worldwide.[1] According to data from the Global Cancer Observatory (GLOBOCAN) in 2022, lung cancer cases have risen, representing approximately 2.5 million new cases, or 12.4% of all cancers types.[2] In Indonesia, lung cancer is also one of the leading cancers in terms of incidence and mortality, with over 38,904 new cases and 34,339 deaths, making it the leading cause of cancer-related deaths (14.1%) in 2022.[3] Furthermore, a report from BPJS Kesehatan indicates that collected in 2018, the total expenditure on cancer treatment reached IDR 1.4 billion, with the proportion of direct medical costs per patient being 50.3% for males and 49.7% for females.[4] These data show that lung cancer not only affects individual health but also places a significant burden on the national healthcare system.

*Corresponding author. E mail: ikhwandichn@med.unismuh.ac.id

Tel: +62-813-5188-6188

Citation: Nugraha IC and Febriza A. Molecular Docking and Dynamics Simulation of *Holothuria scabra* In Non-Small Cell Lung Cancer Through Inhibition of EGFR and KRAS Pathways. Trop J Nat Prod Res. 2025; 9(10): 5077 – 5084 https://doi.org/10.26538/tjnpr/v9i10.50

Official Journal of Natural Product Research Group, Faculty of Pharmacy, University of Benin, Benin City, Nigeria

Lung cancer is a malignant disease that begins in the bronchi or lung tissue; it is primarily categorized into two types: small cell lung cancer (SCLC) and non-small cell lung cancer (NSCLC). NSCLC is the most prevalent, accounting for approximately 85% of all lung cancer cases, whereas SCLC accounts for approximately 15%.[5] Current lung cancer treatments include surgery, chemotherapy, radiotherapy, targeted therapy, and immunotherapy. However, these approaches have several limitations, including resistance to therapy, poor prognosis, and high costs. Therapies targeting mutations, such as epidermal growth factor receptor (EGFR), ALK, KRAS, and G12C, have demonstrated improvements in patient outcomes survival.[6] Although effective at extending the life expectancy of patients with advanced-stage cancer, these treatments face challenges, such as drug resistance, which reduces their long-term effectiveness. Therefore, there is an urgent need for new therapeutic agents that are effective and target specific mechanisms of NSCLC.

Mutations in the EGFR are among the most important and commonly seen genetic changes, acting as key driver mutations in NSCLC. EGFR is a transmembrane protein that functions as a tyrosine kinase receptor for various ligands, playing a crucial role in controlling cell growth, differentiation, and survival.[7] Additionally, KRAS mutations are present in approximately 40% of NSCLC cases, with the KRAS G12C variant being the most prevalent subtype, accounting for approximately 10%–13% of all NSCLC cases.[8] With over 17,000 islands, Indonesia is the largest archipelagic country in the world. About 70% of its territory consists of oceans, and its coastline extends more than 81,000 kilometers, making it the country with the second-longest coastline in the world, after Canada.[9] The province of South Sulawesi, for instance, is abundant in marine natural resources. The sea cucumber is a highly nutritious marine resource with medicinal properties. *Holothuria scabra* (commonly known as sandfish) is a species of sea cucumber found around Sulawesi. A study published in SAGE Open Medicine

reported that extract from *H. scabra* exhibits significant anti-proliferative and anti-inflammatory activity against cancer cells.[10] Conventional drug discovery is a lengthy, complex, and expensive process. On average, developing a single new drug costs over 1.8 million US dollars and takes over 12 years from discovery to clinical trials.[11] The exploration of bioactive compounds from *H. scabra* (sandfish) as potential therapeutic agents for NSCLC can be effectively performed using *in silico* methods supported by *in vitro* studies. *In silico* techniques, such as molecular docking and molecular dynamics, enable early prediction of the affinity and stability of interactions between active compounds and key target proteins involved in the development of NSCLC. These methods help identify the most promising therapeutic candidates before moving on to more complex experimental stages.[12,13] The aim of this study was to evaluate the anticancer potential of bioactive compounds from *H. scabra* against NSCLC using *in silico* approaches by targeting the EGFR and KRAS signaling pathways. The specific objectives of this study were to (i) screen bioactive compounds for toxicity, (ii) assess their binding affinity to EGFR and KRAS through molecular docking, and (iii) evaluate the stability of ligand–protein interactions via molecular dynamics simulations. The novelty of this research is that it is the first comprehensive *in silico* study to explore *H. scabra* bioactives as dual inhibitors of EGFR and KRAS, providing new insights into marine-derived therapeutic candidates for NSCLC.

Materials and Methods

The hardware used was a laptop Asus Vivobook Go 14 E1404FA AMD Ryzen 3-7320U RAM 8GB, Windows 10. The software used was *website* ProTox 3.0, PubChem, RCSB, PyRx (Autodock) application, YASARA software, BIOVIA discovery, and KEGG pathway. The test ligands used in this study included Holothurin A (PubChem CID: 23675050), Holothurin B (PubChem CID: 23674754), Holothurinoside C (PubChem CID: 102036379), Scabraside (PubChem CID: 159134), Holothurinoside G (PubChem CID: 102036382), Bivittoside A (PubChem CID: 157053), Cousteside E (PubChem CID: 102234628), Cousteside I (PubChem CID: 102234632), Eicosapentaenoic acid (PubChem CID: 446284), and Nobiliside E (PubChem CID: 102144660), which are bioactive compounds derived from sea cucumbers and can be seen in Table 1, which can be downloaded from PUBCHEM in pdb format.[10] A comparison ligand, Lazertinib (121269225), was used as a positive control.

Table 1: Compound active code and PubChem ID *H. scabra.*

Ligand code (Compound Name)	PubChem ID
Lazertinib	121269225
C1 (Holothurin A)	23675050
C2 (Holothurin B)	23674754
C3 (Holothurinoside C)	102036379
C4 (Scabraside)	159134
C5 (Holothurinoside G)	102036382
C6 (Bivittoside A)	157053
C7 (Cousteside E)	102234628
C8 (Cousteside I)	102234632
C9 (Eicosapentaenoic acid)	446284
C10 (Nobiliside E)	102144660

Ligand Preparation
Bioactive ligands of sea cucumbers were determined based on research conducted by Wargasetia *et al*., Caulier *et al*., and Mitu *et al* (Table 1).[10] The two-dimensional (2D) structure of the active compound was obtained from the PubChem database (https://pubchem.ncbi.nlm.nih.gov/).[14] After the ligands were obtained, the three-dimensional (3D) structure of each peptide was downloaded from the PUBCHEM website and visualized using the Discovery Studio's BIOVIA software.[15] Subsequently, all ligands were prepared using the PyRx software.

Target Protein Preparation
Target proteins were selected from the literature and analysis of various NSCLC pathogenesis and pathophysiology pathways. Data on several crucial NSCLC pathogenesis and pathophysiology pathways were retrieved from the KEGG pathway website *(https://www.kegg.jp/).* Based on these data, the EGFR [PDB ID: 2ITY] and KRAS [PDB ID: 7LGI] proteins play important roles in NSCLC proliferation and apoptosis.[7] The structure of the selected target protein can be downloaded from the RCSB website *(http://www/rcsb.org).* Each target protein was then cleaned using the BIOVIA Discovery Studio's software.

Toxicity Prediction Test
The toxicity of compounds from sand sea cucumbers (*H. scabra*) was predicted using the Protox Web Server, which is freely accessible at http://tox.charite.de. Protox is a virtual platform that analyzes the toxicity of small chemical compounds.[16,17] The process begins by opening the ProTox website and selecting the "TOX PREDICTION" menu in the menu bar to be directed to the prediction page. In the "PubChem-Name" field, the name of the compound to be tested is entered. Once the compound is found, its 2D structure will appear in the workspace. Next, all available prediction models in the "additional models" section should be activated, and the "start tox-prediction" button in the bottom right should be clicked. After a few moments, the system will display the prediction results, including the LD_{50} value, average similarity, and prediction accuracy level.

Molecular Docking
Docking assays were performed using PyRx software. This process was performed by arranging the grid boxes to correspond to the ATP-binding pocket location on each predetermined target protein.[18] Grid box adjustments were made via the Site Vina Wizard feature in PyRx, with reference to the amino acid residues that form the ATP-binding pocket of each protein (Table 2).[19] Once the setup was completed, the docking process was initiated clicking "Start," then selecting "Add Ligand" to include the ligand to be tested, followed by selecting "Add Macromolecules" to add the target protein, and finally clicking "Forward" and "Run." After obtaining the docking results, the data were saved in a .sdf file format.

Table 2: Amino acid residues of ATP-binding pocket protein

Protein target	ATP-binding pocket
EGFR	LEU718, VAL725, ALA743 , LYS745, GLU762, LEU788, GLN791, MET793, PRO794, GLY796, LEU844
KRAS	GLY13, VAL14, GLY15, LYS16, SER17, ALA18, PHE28, VAL29, ASP30, TYR32, PRO34, ASN116, LYS117, ALA146, LYS147

Visualization of 2D and 3D Structures of Ligand–Protein Complexes
The molecular docking results obtained in the previous stage were visualized using the PyRx application.[20] The docking result file, saved in .sdf format, can be opened by selecting File > Open and then selecting the desired file. Once the 3D view of the ligand–protein complex

ISSN 2616-0684 (Print)
ISSN 2616-0692 (Electronic)

appears, click "Show 2D Interaction" to display the structure and type of binding interaction between the ligand and protein.

Molecular Dynamics

To assess the stability of the complex from the best conformation identified during molecular docking, further analysis was performed using molecular dynamics simulations with YASARA Structure software.[21,22] The molecular dynamics simulation was performed using the Amber14 force field with periodic boundary conditions.[23] The system was maintained at a temperature of 310 K and a physiological pH of 7.4. Solvation was performed using the TIP3P water model, and counterions (Na^+, Cl^-) were added to neutralize the overall charge.[24] The simulation was run for 100 ns with a time step of 0.25 fs. Trajectory data were recorded every 25 ps and then analyzed to calculate the root mean square deviation (RMSD), root mean square fluctuation (RMSF), and the radius of gyration (RG).

Data Analysis

Ligands resulting from de novo modeling were selected based on toxicity.[25] The selected ligands were then analyzed through molecular docking against the EGFR and KRAS target proteins, which are involved in cell cycle progression and apoptosis. The binding scores were compared with those of Lazertinib as a control ligand. The lower binding score of Lazertinib indicates the potential of the ligand as a candidate cell cycle inhibitor and antiapoptotic agent in NSCLC.[26] Ligand–protein interactions were examined based on bond type and residue similarity to Lazertinib, suggesting its function as a competitive inhibitor. Subsequently, the optimal complex was studied through molecular dynamics simulations using YASARA. The analyzed parameters included RG, RMSD, and RMSF.

Results and Discussion

Toxicity Prediction Test

Toxicity prediction tests were conducted using ProTox 3.0 website. The results indicated that all compounds from the sand sea cucumber *H. scabra* were nontoxic, as shown in Tables 3 and 4. Predicting toxicity is a crucial part of drug research and development to ensure safety for clinical use.[27] Based on analysis using the ToxinPred website (https://tox.charite.de/protox3/), all ligands from the *H. scabra* were predicted to be nontoxic. In this virtual toxicity test, the Protox Web Server was used to estimate various toxicological parameters, including acute toxicity, hepatotoxicity, carcinogenicity, immunotoxicity, and cytotoxicity, as well as the potential adverse effects on specific toxicological pathways and targets. The prediction results revealed that compounds C1, C2, C3, C4, C5, C6, C7, C8, and C10 were categorized under toxicity class 5, whereas C9 was classified under class 6, which represents the safest toxicity prediction. For comparison, Lazertinib was classified under class 4. According to the Protox Web Server, the lower the toxicity class number, the higher the compound's potential toxicity. Conversely, the higher the class number, the lower or safer the compound's toxicity level.

Based on the prediction results for target organs, compounds C1, C2, C3, C4, C5, C6, C7, C8, and C10 showed potential toxic effects on the immune system. Meanwhile, Lazertinib, as a control ligand, was predicted to have toxic effects on the immune system and to be carcinogenic. In contrast, compound C9 did not show toxic effects on target organs in the virtual prediction. Therefore, the active compounds from *H. scabra* generally have a safer toxicity profile than Lazertinib.

Table 3: Toxicity prediction results

Compound	LD_{50} mg/kg	Predicted Toxicity Class	Similarity	Accuracy
Lazertinib	1000	4	40.37%	54.26%
C1	3220	5	62.55%	68.07%
C2	3220	5	62.63%	68.07%
C3	4000	5	81.75%	70.97%
C4	2190	5	59.25%	67.38%
C5	4000	5	81.75%	70.97%
C6-	4000	5	83.57%	70.97%
C7	4000	5	82.65%	70.97%
C8	4000	5	82.99%	70.97%
C9	10000	6	100%	100%
C10	4000	5	62.56%	68.07%

Table 4: Organ toxicity results

Compound	Hepatotoxicity	Carcinogenicity	Immunotoxicity	Cytotoxicity
Lazertinib	Inactive	Active	Active	Inactive
C1	Inactive	Inactive	Active	Inactive
C2	Inactive	Inactive	Active	Inactive
C3	Inactive	Inactive	Active	Inactive
C4	Inactive	Inactive	Active	Inactive
C5	Inactive	Inactive	Active	Inactive
C6	Inactive	Inactive	Active	Inactive
C7	Inactive	Inactive	Active	Inactive
C8	Inactive	Inactive	Active	Inactive

ISSN 2616-0684 (Print)
ISSN 2616-0692 (Electronic)

C9	Inactive	Inactive	Inactive	Inactive
C10	Inactive	Inactive	Active	Inactive

Molecular Docking

The molecular docking results between active compounds from *H. scabra* and the EGFR protein showed that compounds C3, C8, and C5 have potential as competitive inhibitor candidates against Lazertinib on the EGFR protein (Table 5). This potential is supported by their lower binding affinity values compared with Lazertinib, the control ligand (−5.2 kcal/mol). Compound C3 binds at the Lazertinib binding site with an affinity of −9.4 kcal/mol, followed by C8 with the same value (−9.4 kcal/mol) and C5 with −8.9 kcal/mol. Overall, all active compounds from *H. scabra* exhibited stronger binding affinities than Lazertinib. However, two compounds, C10 and C1, showed higher (weaker) binding affinity values compared with the control ligand Lazertinib, indicating a lower potential as competitive inhibitors. EGFR activity is a major genetic factor contributing to lung cancer. It is typically caused by mutations in the EGFR tyrosine kinase receptor, resulting in excessive and uncontrolled activation, which can lead to lung cancer progression. To address this condition, various tyrosine kinase inhibitors have been developed specifically for lung cancers with EGFR mutations.[28]

Table 5: Docking results between the *H. scabra* ligand and the EGFR target protein.

Compound	PubChem id	Docking results (Kcal/mol)	RMSD (Å)
Lazertinib	121269225	-5.2	0.0
C3	102036379	-9.4	0.0
C8	102234632	-9.4	0.0
C5	102036382	-8.9	0.0
C4	159134	-7.9	0.0
C6	157053	-7.5	0.0
C7	102234628	-7.0	0.0
C2	23674754	-6.2	0.0
C9	446284	-6.0	0.0
C10	102144660	-3.4	0.0
C1	23675050	3.9	0.0

Based on the results of molecular docking analysis, the active compounds C3, C8, and C5 from *H. scabra* showed potential as competitive inhibitor candidates against Lazertinib targeting the EGFR protein. These three peptides exhibited lower binding affinity values than Lazertinib, along with RMSD values below 2 Å, indicating good binding stability. The C3 ligand interacted with the amino acid residues VAL726, LYS745, and ASP855, which are also involved in Lazertinib interactions. These findings indicate that the C3 ligand has strong potential as a competitive EGFR protein inhibitor, with a mechanism of action similar to Lazertinib.

The molecular docking results between the active compounds from *H. scabra* and the KRAS protein indicated that compounds C4, C3, and C7 have potential as competitive inhibitors against Lazertinib on the target protein (Table 6). This potential is based on their lower binding affinity values compared with Lazertinib, the control ligand (−5.2 kcal/mol). Compound C4 exhibited the strongest binding affinity at −8.7 kcal/mol, followed by C3 with −8.0 kcal/mol and C7 with −7.8 kcal/mol. Overall, most active compounds from *H. scabra* demonstrated stronger binding affinities than Lazertinib. However, compound C1 had a higher (weaker) binding affinity value compared with Lazertinib, indicating a lower potential as a competitive KRAS inhibitor.

Table 6: Docking results between the *H. scabra* ligand and the KRAS target protein.

Compound	PubChem id	Docking results (Kcal/mol)	RMSD (Å)
Lazertinib	121269225	-4.8	0.0
C4	159134	-8.7	0.0
C3	102036379	-8.0	0.0
C7	102234628	-7.8	0.0
C8	102234632	-7.5	0.0
C5	102036382	-6.7	0.0
C9	446284	-6.5	0.0
C6	157053	-6.1	0.0
C2	23674754	-5.4	0.0
C10	102144660	-5.2	0.0
C1	23675050	-2.7	0.0

ISSN 2616-0684 (Print)
ISSN 2616-0692 (Electronic)

KRAS is part of the human RAS (rat sarcoma viral oncogene homolog) gene family; it is frequently mutated in several types of cancer, including pancreatic ductal adenocarcinoma (PDAC), colorectal cancer (CRC), and NSCLC. In lung cancer, activating KRAS mutations are among the most common oncogenic drivers, occurring in approximately 20%–30% of cases.[29] Furthermore, mutations in the KRAS gene, a member of the RAS family, constantly activate oncogenes and inhibit apoptosis while contributing to cancer cell growth. This occurs by increasing the levels of antiapoptotic proteins, such as Bcl-xL and survivin, and reducing the levels of proapoptotic proteins, such as TDG and TRAIL.[30] In this way, KRAS promotes therapy resistance and worsens the prognosis for cancer.

The molecular docking analysis indicated that the active compounds C4, C3, and C7 from *H. scabra* have potential as competitive inhibitors against Lazertinib on the KRAS protein. These three ligands showed binding affinity values of −8.7 kcal/mol (C4), −8.0 kcal/mol (C3), and −7.8 kcal/mol (C7), which are stronger than those of ATP, the natural ligand (−4.8 kcal/mol). In addition, all ligands had RMSD values below 2 Å, suggesting solid binding stability. Ligands C4 and Lazertinib also displayed similar interactions with two amino acid residues, LYS117 and LYS147, indicating that C4 could inhibit Lazertinib binding to KRAS. However, both ligands are predicted to have toxic effects on the immune system; therefore, further research is necessary before they can be considered for clinical use in humans.

Visualization of Molecular Docking

In interactions with EGFR, Lazertinib and compound C3 bind to the key residues ASP855, LYS745, and VAL726 through hydrogen bonds and hydrophobic interactions. This similarity in binding sites indicates that C3 can potentially mimic the mechanism of Lazertinib for inhibiting EGFR activity, especially because ASP855 and LYS745 are crucial residues within the tyrosine kinase domain involved in phosphorylation. In KRAS, Lazertinib and compound C4 interact with LYS117 and LYS147 residues via hydrogen bonds and Pi-alkyl interactions. The similarity in these residues indicates that C4 may bind to KRAS at the same critical site as Lazertinib, possibly inhibiting KRAS function in cell proliferation and signal transduction. Therefore, the shared binding residues between the test ligands and Lazertinib for EGFR and KRAS highlight the potential of these ligands to effectively inhibit the functions of both target proteins (Table 7 and Figure 1).

Table 7: Types of interactions and similarities of amino acid residues resulting from molecular docking

Ligand-Protein	Types of Interactions	Amino Acid Residues
Lazertinib-EGFR	Van der Waals	LYS745*
	Carbon hydrogen bond	ASP855*
	Pi-cation	LYS728
	Pi-Sigma	VAL726*
	Pi-Alkyl	LEU718, LEU792, LEU844
C3-EGFR	Van der Waals	-
	Conventional hydrogen bond	ASP855*, LYS745*
	Alkyl	VAL726*
	Pi-Alkyl	ALA722, CYS797, PHE723, LEU747
Lazertinib-KRAS	Van der Waals	-
	Conventional hydrogen bond	ASP30, ASN85
	Carbon hydrogen bond	-
	Pi-cation	LYS117**
	Pi-Alkyl	LEU120, LYS147**
C4-KRAS	Van der Waals	-
	Conventional hydrogen bond	LYS16, GLU31, TYR32, LYS117**, ALA146
	Carbon hydrogen bond	GLY15
	Alkyl	-
	Pi-Alkyl	PHE28, LYS147**

Description: *Same amino acid residue as EGFR, **Same amino acid residue as KRAS

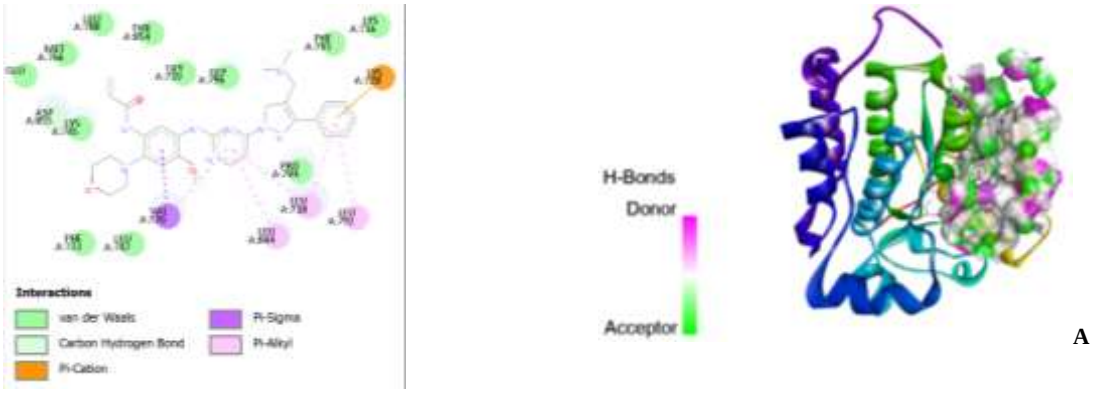

A

ISSN 2616-0684 (Print)
ISSN 2616-0692 (Electronic)

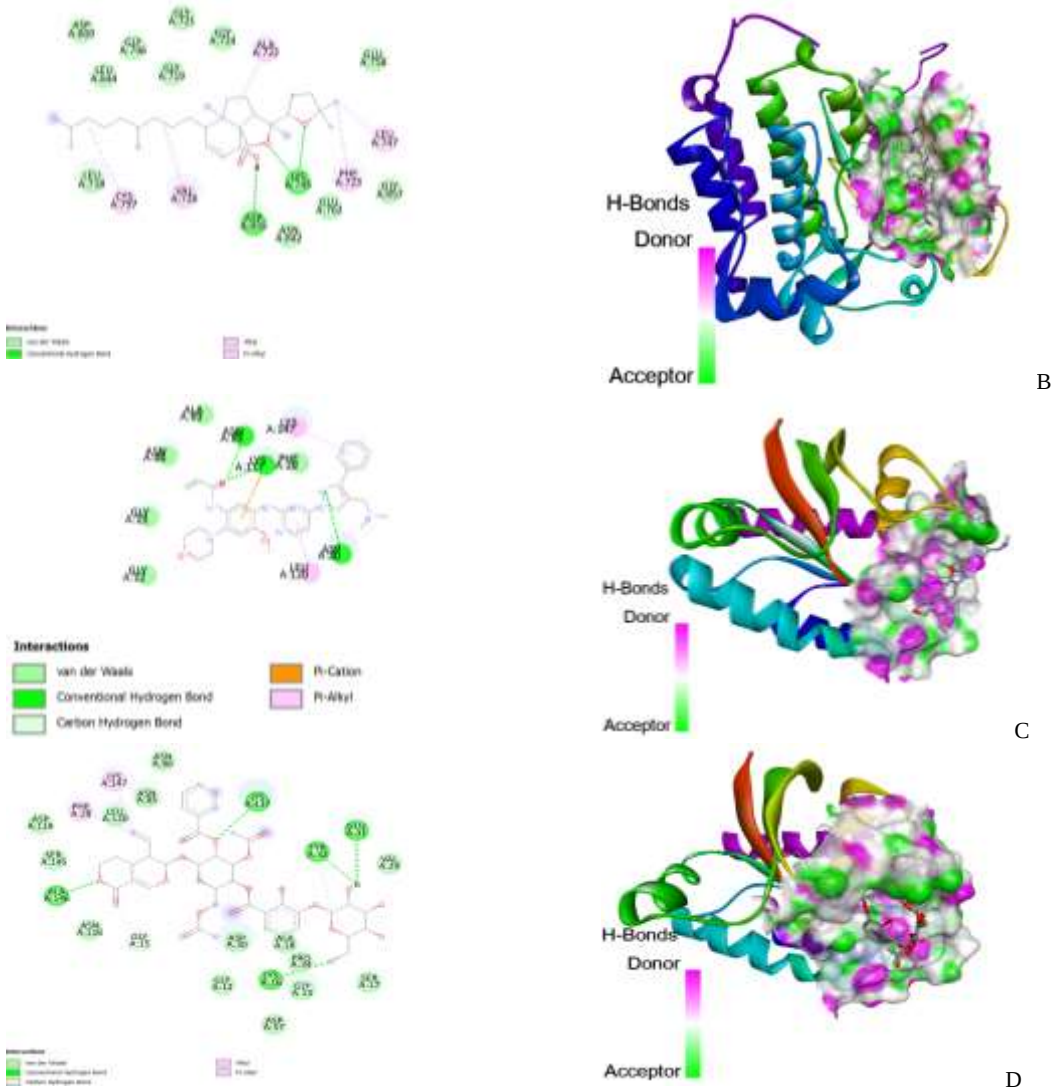

Figure 1: Visualization of molecular docking interaction results for ligand–protein complexes. A: Lazertinib–EGFR(2D/3D); B: C3–EGFR (2D/3D); C: Lazertinib–KRAS (2D/3D); D: C4–KRAS (2D/3D).

Molecular Dynamics

Molecular dynamics simulations were conducted for 100 ns, focusing on the Lazertinib, C3, and C4 ligand complexes, which served as positive controls. These ligands were docked into the EGFR and KRAS active sites. They were chosen based on their lower binding energies compared with other ligands evaluated during the molecular docking analysis. The RG measures the overall equilibrium conformation of a protein system. Lower values indicate a folded protein, whereas higher values indicate an unfolded state.

Figure 2A displays the RG profiles of EGFR in complex with Holothurinoside C and Lazertinib over a 100 ns simulation. Both complexes remained fairly stable, fluctuating within a narrow range of approximately 20.2–21.3 Å. Holothurinoside C showed slightly more variation, with an average RG of 20.8 Å compared with Lazertinib's 20.6 Å, though the differences were minimal. These results suggest that the overall compactness of the EGFR–ligand complexes was preserved, indicating no significant structural disturbance upon ligand binding. Figure 2B shows the RMSD profiles of EGFR complexes, indicating that both systems reached equilibrium within the first 10–20 ns. The EGFR–Holothurinoside C complex fluctuated between 2.5–4.8 Å (average, 3.5–4.0 Å), whereas the EGFR–Lazertinib complex maintained slightly lower deviations of 1.7–3.4 Å (average, 2.5–3.0 Å). Although Holothurinoside C had marginally higher RMSD values, the differences were not significant enough to indicate structural instability, implying that both complexes remained stable throughout the simulation. Figure 2C displays the residue-wise RMSF profiles of EGFR complexes, showing that most residues fluctuated within 1–4 Å, with the terminal regions exhibiting higher peaks of 8–12 Å. Holothurinoside C and Lazertinib exhibited similar fluctuation patterns, with only minor deviations in certain loop regions. These results suggest that ligand binding did not cause major changes in EGFR flexibility, and the overall residue mobility remained within normal dynamic ranges.

Figure 2D–F shows the structural stability and flexibility analyses of KRAS when bound to Lazertinib and Scabraside. The RG values (Figure 2D) were similar for both ligands, ranging from 15.2 to 17.6 Å with averages around 15.8–16.2 Å, indicating that KRAS remained compact and structurally stable.[31,32] The RMSD plots (Figure 2E) showed that Lazertinib remained stable within 5–7 Å after equilibrium, whereas Scabraside generally had lower deviations (2–5 Å) but experienced a temporary spike up to 10–11 Å between 60 and 80 ns, indicating brief conformational changes or ligand reorientation.[33] Despite this fluctuation, Scabraside maintained overall stable interactions with KRAS. Residue-wise flexibility profiles (Figure 2F) revealed that most residues fluctuated between 0.5 and 3.5 Å for both ligands, with terminal regions reaching 6–7 Å. Although Scabraside showed slightly higher flexibility at some sites, the patterns were mostly similar, implying that it may subtly affect local dynamics without significantly disrupting KRAS structure.

ISSN 2616-0684 (Print)
ISSN 2616-0692 (Electronic)

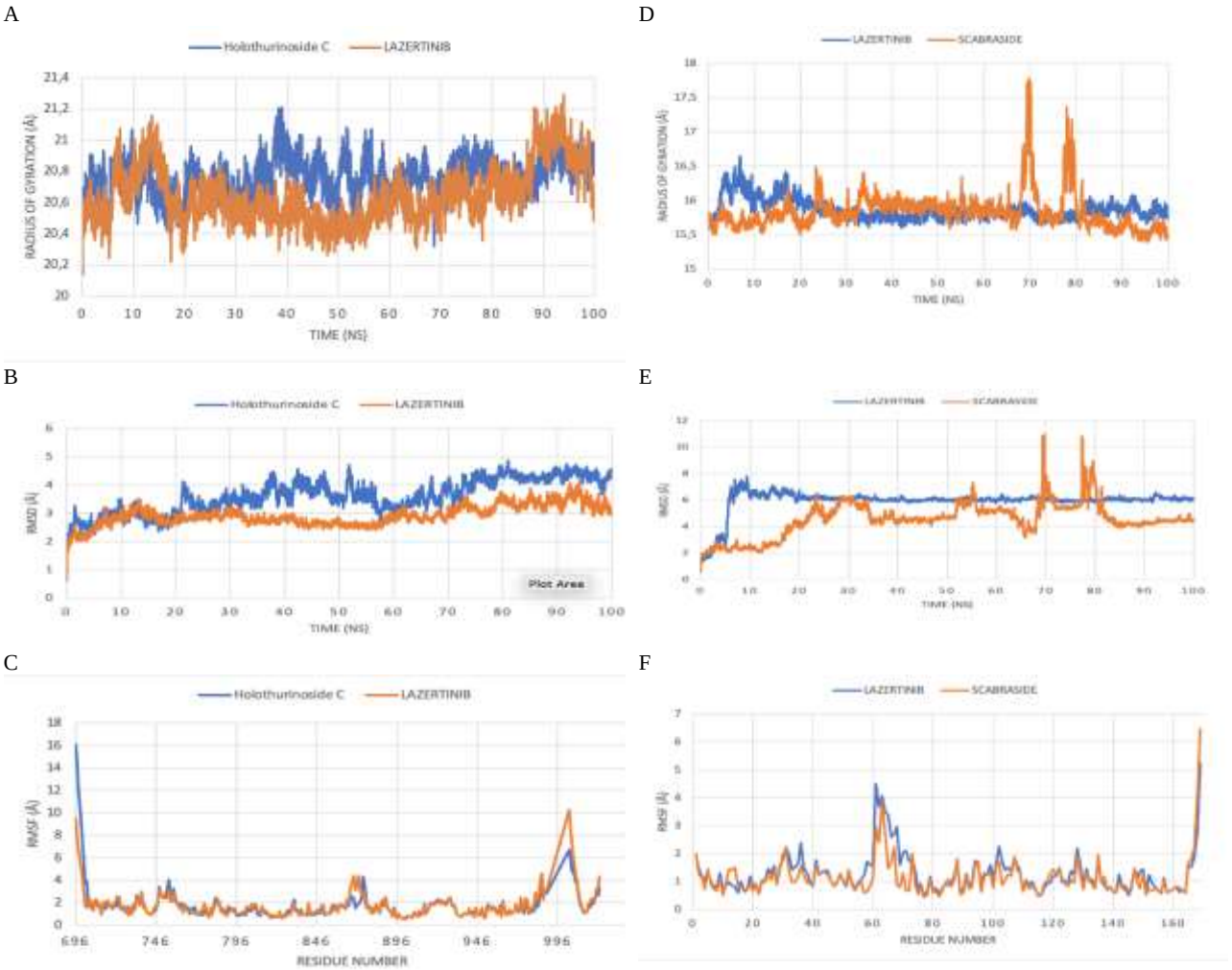

Figure 2: Structural stability analysis of EGFR and KRAS ligand complexes during 100 ns molecular dynamics simulations. A: Radius of gyration (RG) plot of EGFR; B: Root mean square deviation (RMSD) plot of EGFR; C: Root mean square fluctuation (RMSF) plot of EGFR; D: Radius of gyration (RG) plot of KRAS; E: Root mean square deviation (RMSD) plot of KRAS; F: Root mean square fluctuation (RMSF) plot of KRAS complexes.

Conclusion

Based on the results of the research, it can be concluded that all tested ligands showed nontoxic properties according to the toxicity prediction analysis. Furthermore, ligands C3 and C4 derived from *H. scabra* (sandfish) demonstrated potential as inhibitors of cancer cell cycle proliferation in NSCLC through *in silico* methods using molecular docking and molecular dynamics simulation. Both acted as competitive EGFR protein inhibitors, which is the target of the drug Lazertinib. Furthermore, ligand C4 also showed potential as a competitive KRAS protein inhibitor, which plays a role in regulating the anti-apoptotic pathway in lung cancer cells. Therefore, the active compounds C3 and C4 from *H. scabra* hold promising potential for further development as alternative therapeutic candidates for NSCLC treatment.

Conflict of Interest

The authors declare no conflicts of interest

Authors' Declaration

The authors hereby declare that the work presented in this article is original and that any liability for claims relating to the content of this article will be borne by them.

Acknowledgements

The authors gratefully acknowledge the Laboratory of Chemistry, Faculty of Pharmacy, Hasanuddin University, for supporting this research.

References

1. Nurcahyanti ADR, Tenia TF, Candra F. PTEN-Akt/mTOR expression level in A549 lung cancer cells in response to cisplatin, carotenoids, and their combination. Trop J Nat Prod Res. 2024;8(1):5774–5778.
2. Bray F, Laversanne M, Sung H, Ferlay J, Siegel RL, Soerjomataram I, Jemal A. Global cancer statistics 2022: GLOBOCAN estimates of incidence and mortality worldwide for 36 cancers in 185 countries. CA Cancer J Clin. 2024;74(3):229–263.
3. Ji Yuting Ji, Yunmeng Zhang, Siwen Liu, Jingjing Li, Qianyun Jin, Jie Wu, Hongyuan Duan, Xiaomin Liu, Lei Yang, Yubei Huang. The epidemiological landscape of lung cancer: current status, temporal trend and future projections based on the latest estimates from GLOBOCAN 2022. J Natl Cancer Cent. 2025;5(3):278–286.

4. Andriani Y, Kristina SA, Wiedyaningsih C. Estimation of direct medical cost (DMC) of cancer in Indonesia. Majalah Farmaseutik. 2021;17(3):251–255.
5. Alduais Y, Zhang H, Fan F, Chen J, Chen B. Non-small cell lung cancer (NSCLC): a review of risk factors, diagnosis, and treatment. Medicine (Baltimore). 2023;102(8):e32899.
6. Kirubhanand C, Merciline Leonora J, Anitha S, Sangeetha R, Nachammai KT, Langeswaran K, Gowtham Kumar S. Targeting potential receptor molecules in non-small cell lung cancer (NSCLC) using in silico approaches. Front Mol Biosci. 2023;10:1124563.
7. Melosky B, Kambartel K, Häntschel M, Bennetts M, Nickens DJ, Brinkmann J, Kayser A, Moran M, Cappuzzo F. Worldwide prevalence of epidermal growth factor receptor mutations in non-small cell lung cancer: a meta-analysis. Mol Diagn Ther. 2022;26(1):7–18.
8. Lim TKH, Skoulidis F, Kerr KM, Novello S, Dooms C, Shames DS, Tan DS-W, Lopes G, Vansteenkiste J, Dingemans A-MC, Ahn M-J, de Marinis F. KRAS G12C in advanced NSCLC: prevalence, co-mutations, and testing. Lung Cancer. 2023;184:107293. doi:10.1016/j.lungcan.2023.107293.
9. Sains R, Kelautan DT, Sultan D, Muhammad D, Ramadhan F. The Role of Government Policies in Managing Indonesia's Marine Resources. Marine Science and Technology Research. 2024;7(1):34–40.
10. Wargasetia TL, Ratnawati H, Widodo N, Widyananda MH. Antioxidant and anti-inflammatory activity of sea cucumber (*Holothuria scabra*) active compounds against KEAP1 and iNOS protein. Bioinform Biol Insights. 2023;17:1–12
11. Shaker B, Ahmad S, Lee J, Jung C, Na D. In silico methods and tools for drug discovery. Comput Biol Med. 2021;137:104851.
12. Zare A, Izanloo S, Khaledi S, Ahmadi M, Hosseini SA, Asadzadeh Z, Khazaei S, Ferns GA, Avan A, Soleimanpour S. A bibliometric and in silico-based analysis of anti-lung cancer compounds from sea cucumber. Mar Drugs. 2023;21(5):281.
13. Hossain A, Dave D, Shahidi F. Antioxidant potential of sea cucumbers and their beneficial effects on human health. Mar Drugs. 2022;20(8):521.
14. Diningrat S, Diky MEK. Anti-acne and antibacterial bioactivity properties of teak (Tectona grandis) flower essential oil. Trop J Nat Prod Res. 2023;7(11):2001–2006.
15. Hardono H, Soetrisno S, Purwanto B, Wasita B, Nurwati I, Pamungkasari P. In silico study of the antidiabetic effect of ethyl acetate fraction of banana bract in diabetic rats. Trop J Nat Prod Res. 2024;8(11):1029–1036. doi:10.26538/tjnpr/v8i11.7.
16. Banerjee P, Kemmler E, Dunkel M, Preissner R. ProTox-3.0: a webserver for the prediction of toxicity of chemicals. Nucleic Acids Res. 2024;52(W1):W513–W520.
17. Makiyah NN, Sri USD. In silico toxicity prediction of bioactive compounds of *Dioscorea alata L.*. Trop J Nat Prod Res. 2022;6(10):1587–1596.
18. Xu X, Huang M, Zou X. Docking-based inverse virtual screening: methods, applications, and challenges. Biophys Rep. 2018;4(1):1–16.
19. Agu PC, Afiukwa CA, Orji OU, Ezeorba TP, Agu CM, Nwankwo AP, Ugwuoke CE, Okpala OE, Chukwudozie KI, Okereke OE, Onoh UE, Ani OC, Onwe CS, Ogugua VN, Egba SI. Molecular docking as a tool for the discovery of molecular targets of nutraceuticals in disease management. Sci Rep. 2023;13(1):13398.
20. Ayu Kartika W, Affan Silalahi A, Rambe R, Putra Fattara F. Molecular docking of meniran (*Phyllanthus niruri L.*) against tyrosine kinase inhibition as an anticancer agent. Indones J Pharm Clin Res. 2024;7(2):14–024.
21. Ouassaf M, Belaidi S, Mogren Al-Mogren M, Chtita S, Ullah Khan S, Thet Htar T. Combined docking methods and molecular dynamics to identify effective antiviral 2,5-diaminobenzophenone derivatives against SARS-CoV-2. J King Saud Univ Sci. 2021;33(2):101352.
22. Yuli Astuti PD, Fadilah F, Promsai S, Bahtiar A. Integrating molecular docking and molecular dynamics simulations to evaluate active compounds of *Hibiscus schizopetalus* for obesity. J Appl Pharm Sci. 2024;14(06):070–078.
23. Wang J, Wolf RM, Caldwell JW, Kollman PA, Case DA. Development and testing of a general amber force field. J Comput Chem. 2004;25(9):1157–1174.
24. Mark P, Nilsson L. Structure and dynamics of the TIP3P, SPC, and SPC/E water models at 298 K. J Phys Chem A. 2001;105(43):9954–9960.
25. Deka A, Saikia V. Prediction of ACE-inhibitory and antioxidant peptides from storage proteins of edible seeds and nuts using in silico approaches. Sustain Food Proteins. 2023;1(2):84–98.
26. Widyananda MH, Pratama SK, Samoedra RS, Sari FN, Kharisma VD, Ansori ANM, Antonius Y. Molecular docking study of sea urchin (*Arbacia lixula*) peptides as multi-target inhibitors for non-small cell lung cancer (NSCLC) associated proteins. J Pharm Pharmacogn Res. 2021;9(4):484–496.
27. Zhang R, Wen H, Lin Z, Li B, Zhou X. Artificial intelligence-driven drug toxicity prediction: advances, challenges, and future directions. Toxics. 2025;13(7):525.
28. Swiatnicki MR, Rennhack JP, Ortiz MMO, Yoshida K, Yao L, Zeng Q, Crouch J, Crespo VO, Wang Y, Ball D, Stevenson S, Gan C, Singh S, Asara JM, Janne PA, Solomon B, Sato M, Janne P, Bivona TG. Elevated phosphorylation of EGFR in NSCLC due to mutations in PTPRH. PLoS Genet. 2022;18(9):e1010362.
29. Santarpia M, Ciappina G, Spagnolo CC, Squeri A, Passalacqua MI, Aguilar A, Gonzalez-Cao M, Giovannetti E, Silvestris N, Rosell R. Targeted therapies for KRAS-mutant non-small cell lung cancer: from preclinical studies to clinical development a narrative review. Transl Lung Cancer Res. 2023;12(2):346–368.
30. Ferreira A, Pereira F, Reis C, Oliveira MJ, Sousa MJ, Preto A. Crucial Role of Oncogenic KRAS Mutations in Apoptosis and Autophagy Regulation: Therapeutic Implications. Cells. 2022;11(14):2183.
31. Paul SK, Saddam M, Tabassum N, Hasan M. Molecular dynamics simulation of wild and mutant proteasome subunit beta type 8 (PSMB8) protein: implications for restoration of inflammation in experimental autoimmune encephalomyelitis pathogenesis. Heliyon. 2025;11(1):e41166.
32. Koshy C, Parthiban M, Sowdhamini R. 100 ns molecular dynamics simulations to study intramolecular conformational changes in Bax. J Biomol Struct Dyn. 2010;28(1):71–83.
33. Fatriansyah JF, Boanerges AG, Kurnianto SR, Pradana AF, Fadilah, Surip SN. Molecular dynamics simulation of ligands from *Anredera cordifolia* (binahong) to the main protease (Mpro) of SARS-CoV-2. J Trop Med. 2022;2022:1178228.